AIAA JOURNAL
Vol. 36, No. 2, February 1998

Interfacing of Fluid and Structural Models via Innovative Structural Boundary Element Method

P. C. Chen* and I. Jadic†
ZONA Technology, Inc., Mesa, Arizona 85202

An innovative structural boundary element method (BEM) solver is developed for interfacing the computational fluid dynamics (CFD) and computational structural dynamics (CSD) grids. Formulated as a solid mechanics problem with a minimum strain energy requirement, the BEM solver generates a truly three-dimensional universal spline matrix. The universal spline matrix is a vector operator that includes the coupling of displacements and forces along all axes. Based on a similar formulation, an exterior BEM solver is also developed to account for the flowfield grid deformation. Thus, the BEM solver allows a unified treatment of the displacement and force transformation for CFD/CSD interfacing, as well as the computation of the flowfield grid deformation. The solution procedure is fully automated, and no additional model generation is required; therefore, it is ideally suitable for computational aeroelasticity and multidisciplinary optimization applications.

Introduction

AEROELASTIC analysis, as an interdisciplinary problem, requires the coupling of the aerodynamic and structural responses. In practice, the requirements to generate the discretized models of these disciplines are subject to different engineering considerations. The grid of the discretized aerodynamic model is usually placed on the external surface, whereas that of the structural model is placed on the internal load-carry components. This gives rise to the interfacing problem of transferring the computed data between these two grid systems. This interfacing problem usually amounts to the transformation of the displacements computed in the structural grid to the aerodynamic grid and that of loads from the aerodynamic grid to the structural grid. The development of a suitable methodology for solving this type of interfacing problem is by no means a trivial task. In fact, such a methodology should be further developed as the aerodynamic and/or structural methods advance.

In the early 1970s, Harder and Desmarais[1] developed an infinite plate spline (IPS) method, which was a significant improvement over the linear spline methods, e.g., Ref. 2. This development was motivated by the advent of lifting surface methods in aerodynamics, e.g., Ref. 3, which required a two-dimensional interfacing method such as IPS (the two-dimensional surface is defined as the plane of the lifting surface). Later, Appa[4] improved the IPS approach by using a finite surface spline (FSS). Further refinements of the IPS method have been proposed by Duchon,[5] who has provided the groundwork for the thin plate spline (TPS) approach by incorporating some three-dimensional aspects. Other methods are presently available that are compatible with the lifting surface aerodynamics approximation, such as multiquadrics biharmonics.[6] Excellent surveys on the state of the art in this area are by Smith et al.[7] and by Hounjet and Meijer.[8]

However, the situation has changed with the maturation of Computational fluid dynamics (CFD) methods. These methods require an exact description of the surface and are known to be geometry sensitive, e.g., the Navier–Stokes solvers.[8] Consequently, a very accurate mapping of the three-dimensional deformations is necessary, especially for the leading-edge region. It appears obvious that the overall accuracy of the computational aeroelasticity (CAE) application cannot exceed that of the information transfer methodology. In other words, the use of high-performance CFD and computational structural dynamics (CSD) codes is warranted only if the interfacing algorithm provides an equivalent level of accuracy.

The situation concerning the use of classical interpolation techniques, e.g., IPS,[1] to three-dimensional bodies is altogether unclear. Several extensions may be quoted that have broadened the scope of these procedures, e.g., Ref. 5, but the basic assumption of uncoupled displacements still remains. The lack of coupling implies that there is no interaction between the displacements acting along different axes. Subsequent examples that show the errors incurred by such an assumption for truly three-dimensional bodies are included.

A major difficulty in the CFD/CSD interfacing problem is the lack of similarities between the aerodynamic (CFD) and structural (CSD) models. In engineering practice it may be required to interface a simplified CSD model such as a beam for the fuselage with a three-dimensional CFD model. Further, some components may be present in one of the models, but not in the other. For example, an underwing store may be modeled as a point mass for CSD purposes, but its surface may require a detailed CFD discretization. Other difficult situations that may be encountered involve the treatment of control surface displacements, i.e., slope discontinuities, which usually lead to zoning requirements. This requires engineering judgment and experience, being user-interaction intensive. In this respect, a different class of methods is available that uses specialized identification procedures to obtain the aeroelastic model, e.g., ELFINI (Ref. 9). The main disadvantage of such an approach is the inherent high cost (especially in terms of engineering effort) implied by a third model identification procedure, which has to be validated in addition to the structural (CSD) and aerodynamics (CFD) computations.

Finally, it will be noted that some of the IPS methods exhibit unfavorable characteristics for extrapolation due to the zero slope boundary condition at infinity.

Another type of problem that will be addressed herein concerns the deformation of the CFD flowfield grid to accommodate for the change of shape in the fluid–structure interface. Some CFD applications circumvent this problem by using the transpiration boundary conditions.[8] For exact boundary conditions treatment, the flowfield grid deformation problem has been tackled by either regenerating the grid at each time step, e.g., by Guruswamy,[10] or by considering the supplementary problem of a network of springs with the nodes located at the CFD grid points, e.g., by Batina.[11]

Here, an innovative approach is introduced to solve the CFD/CSD interfacing problem. Based on the elastostatics boundary element method (BEM), a BEM solver is devised that generates a universal spline matrix $\boldsymbol{S}$ such that

$$\boldsymbol{u}_a = \boldsymbol{S}\boldsymbol{u}_s \tag{1}$$

Received March 20, 1997; presented as Paper 97-1088 at the AIAA/ASME/ASCE/AHS/ASC 38th Structures, Structural Dynamics, and Materials Conference, Kissimmee, FL, April 7–10, 1997; revision received Sept. 17, 1997; accepted for publication Oct. 6, 1997.

*Vice President, 2651 W. Guadalupe Road, Suite B-228. E-mail: zona@indirect.com.

†Member of Technical Staff; currently Senior Engineer, Structural Dynamics, Raytheon Aircraft Co., P.O. Box 85, Wichita, KS 67201-0085.

where $\boldsymbol{u}$ is the displacement vector and the subscripts s and a refer to the structural (CSD) and aerodynamic (CFD) grids, respectively.

Once the universal spline matrix S is generated, one can easily prove, by the principle of virtual work, that the force transformation from CFD to CSD grids is given by

$$f_s = S^T f_a \tag{2}$$

where $\boldsymbol{f}$ is the force vector.

The same elastostatics BEM is applied as an exterior BEM solver to determine the CFD flowfield grid deformation. Therefore, the BEM approach allows a unified treatment of the CFD/CSD interfacing problems.

The major thrust of the present BEM solver lies in the use of a full three-dimensional approach, implying that the displacements and tractions (external loads) along different axes interact with each other, e.g., a displacement along the x axis produces effects along all other axes.

Approach

The CFD/CSD interfacing is treated here as a solid mechanics problem. Many of the interpolation schemes currently in use have been derived on different assumptions that have little to do with the elasticity of the structure examined, e.g., topological methods. Further, these methods claim to be applicable to any smooth data such as temperatures or strains. On the other hand, structural-based methods, such as IPS,[1] FSS,[4] and TPS,[5] make use of the thin plate approximation. As opposed to these, the present approach is based on the full three-dimensional structural equilibrium equations and aimed only at structurally related quantities, i.e., displacements and loads.

The only assumption concerning the relationship between CFD and CSD models is that the CSD grid points are located within or on the surface defined by the CFD surface grid. An equivalent solid mechanics problem is now defined, in which the CFD grid becomes the boundary of a solid body of elastic homogeneous material. For a given deformation prescribed at the internal (CSD) grid points, the interfacing problem becomes how to determine the corresponding deformation on the solid body surface (CFD surface grid; Γ in Fig. 1). This type of problem, involving a homogeneous elastic body, can be solved effectively by the application of the BEM.

Thus, a BEM solver has been developed that provides the solution to the defined solid mechanics problem. Embedding a minimum strain energy requirement, the BEM solver naturally leads to a universal spline matrix that relates the CFD and CSD displacements and forces, Eqs. (1) and (2).

Background of Elastostatics BEM

The starting point for the derivation of the elastostatics BEM equation are the Navier (equilibrium) equations in terms of displacements, which in tensor notation have the form[12]

$$[1/(1-2\nu)]u_{j,jl} + u_{l,jj} = 0 \tag{3}$$

where ν is Poisson's ratio and the body forces have been neglected. Equation (3) applies throughout the volume of a homogeneous body, V (Fig. 2). The usual BEM approach is to obtain an integral form of the equilibrium equations, relating the displacement at any internal point to the values of the displacements $\boldsymbol{u}$ and surface loads p on the boundary Γ (Fig. 2). The result is known as Somigliana's identity, e.g., Ref. 12:

$$u_k^i + \int_\Gamma p_{lk}^* u_k \, d\Gamma = \int_\Gamma u_{lk}^* p_k \, d\Gamma \tag{4}$$

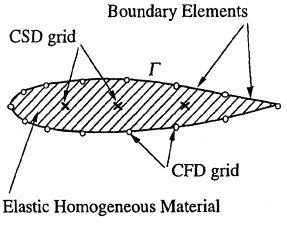

Fig. 1 Internal BEM problem.

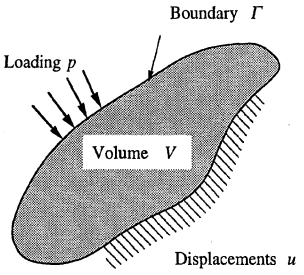

Fig. 2 Structural BEM problem geometry.

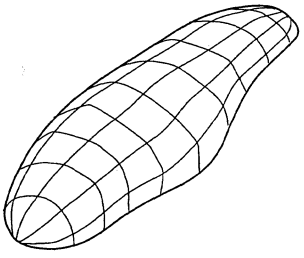

Fig. 3 Discretization of the boundary.

where the superscripts i and $*$ refer to the internal point and Kelvin solutions, respectively.

Next, the boundary of the body Γ (Fig. 3) is discretized into elements denoted as boundary elements. The boundary integral equation (4) can be recast into the following matrix form:

$$\boldsymbol{u}_s + \boldsymbol{H}_{\text{bi}}\boldsymbol{u}_a = \boldsymbol{G}_{\text{bi}}\boldsymbol{p} \tag{5}$$

where the subscript bi is boundary–interior influence. The displacement vectors $\boldsymbol{u}_a$ and $\boldsymbol{u}_s$ in Eq. (5) are given at the boundary (CFD surface grid) and interior (CSD grid) points, respectively.

A special treatment of the boundary integral equation (4) is required for points located on the boundary. In matrix form, the equation that relates the displacements and loads on the boundary is[12]

$$\boldsymbol{H}_{\text{bb}}\boldsymbol{u}_a = \boldsymbol{G}_{\text{bb}}\boldsymbol{p} \tag{6}$$

where the subscript bb refers to boundary–boundary influence.

Substituting Eq. (6) into Eq. (5) yields the elastostatics BEM equation

$$\boldsymbol{u}_s = \boldsymbol{B}\boldsymbol{u}_a \tag{7}$$

where

$$\boldsymbol{B} = \boldsymbol{G}_{\text{bi}}\boldsymbol{G}_{\text{bb}}^{-1}\boldsymbol{H}_{\text{bb}} - \boldsymbol{H}_{\text{bi}}$$

Observe that $\boldsymbol{B}$ in Eq. (7) can be inverted only if the number of internal points is equal to the number of points on the boundary. A least square approach can be utilized in the case where the number of internal points is greater than the number of boundary points. However, in usual engineering applications the CSD grid is much coarser than the CFD surface grid. Therefore, the present BEM solver is defined for the situation when the number of internal (CSD) points is less than the number of boundary (CFD surface) points. To solve Eq. (7) and obtain the universal spline matrix $\boldsymbol{S}$ [see Eqs. (1) and (2)], a BEM solver is developed based on the minimization of the strain energy, as detailed in the following section.

Note that the displacement vectors $\boldsymbol{u}$ in Eq. (7) are fully coupled along all axes and, therefore, the present method is formulated as a vector field, leading to a three-dimensional vector operator.

Minimum Strain Energy Requirement

As discussed in the preceding section, Eq. (7) does not provide enough conditions to relate the displacements at the aerodynamic grid points, $\boldsymbol{u}_a$, to the (given) structural grid displacements $\boldsymbol{u}_s$. Therefore, an additional condition is introduced that minimizes the strain energy function W, defined as

$$W = \int_\Gamma p_k u_k \, d\Gamma \tag{8}$$

The choice of this minimum strain energy requirement ensures that no unwanted deformations appear.

In matrix form, the strain energy function W can be expressed as

$$W = \boldsymbol{u}_a^T \boldsymbol{R}_a \boldsymbol{p} \tag{9}$$

where $\boldsymbol{R}_a$ is a matrix containing the areas of the boundary elements.

From Eqs. (6) and (9) it follows that

$$W = \boldsymbol{u}_a^T \boldsymbol{A} \boldsymbol{u}_a \tag{9a}$$

where

$$\boldsymbol{A} = \boldsymbol{R}_a \boldsymbol{G}_{bb}^{-1} \boldsymbol{H}_{bb}$$

For the given displacements at the structural grid points, the Lagrangian multipliers technique is used to minimize the strain energy W [Eq. (9a)]. Thus, an objective function is defined as

$$F = \boldsymbol{u}_a^T \boldsymbol{A} \boldsymbol{u}_a - \boldsymbol{\lambda}^T (\boldsymbol{u}_s - \boldsymbol{u}_{s,\text{given}}) \tag{10}$$

where $\boldsymbol{u}_{s,\text{given}}$ are the given values of the displacements and $\boldsymbol{\lambda}$ is a vector containing the Lagrangian multipliers. The unknowns to be solved for by minimizing F [Eq. (10)] are the boundary displacements $\boldsymbol{u}_a$ and the Lagrangian multipliers $\boldsymbol{\lambda}$. The singularity present in matrix $\boldsymbol{A}$ can be removed by eliminating the rigid-body degrees of freedom and recovering them from the given structural displacements by means of simple kinematics.

Applying the Lagrangian multipliers technique,

$$\frac{\partial F}{\partial \boldsymbol{u}_a} = 0$$

with the constraint conditions,

$$\boldsymbol{u}_s = \boldsymbol{u}_{s,\text{given}}$$

the desired universal spline matrix $\boldsymbol{S}$ can be obtained:

$$\boldsymbol{u}_a = \boldsymbol{S} \boldsymbol{u}_s \tag{1}$$

Once $\boldsymbol{S}$ is obtained, its transpose can be used directly to transform the forces from the aerodynamic to the structural grid points; see Eq. (2). Figure 4 shows the essential steps for the generation of $\boldsymbol{S}$. First, for a given CFD mesh, a BEM model can be generated automatically by adopting the CFD surface grid as boundary element grid. Then, using the given CSD locations, the formulation described by Eqs. (8–10) together with the minimum strain energy requirement yields the BEM solver universal spline matrix $\boldsymbol{S}$, [Eq. (1)]. The size of the BEM problem represented by the present approach is equal to $3 \times N$, where 3 is the number of degrees of freedom for each grid point (for a three-dimensional problem) and N the number of the CFD grid points. The system solver used must be able to handle full, unsymmetrical matrices. However, its efficiency is not critical for the overall approach because matrix $\boldsymbol{S}$ is invariant in the CFD/CSD aeroelastic time-marching procedure. (It is computed prior to the aeroelastic computation.) $\boldsymbol{S}$ is an operator on the CFD and CSD grid systems and is independent of the actual displacements.

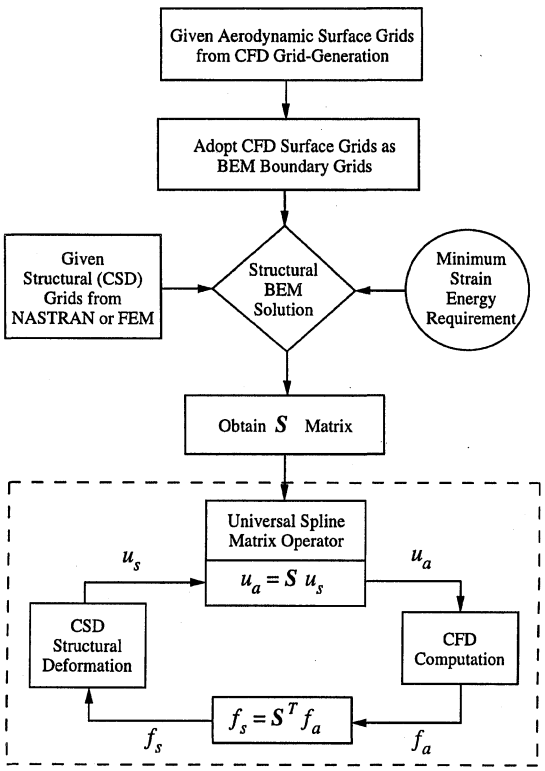

Fig. 4 Flowchart showing BEM technique.

Deformation of CFD Flowfield Grid Using the Exterior BEM Solver

Once the deformation of the CFD surface grid is determined by applying the universal spline matrix $\boldsymbol{S}$ [Eq. (1)], the CFD computation requires the flowfield grid to deform accordingly. Two basic conditions that have to be satisfied by the deformed flow-field grid are as follows: 1) the deformations should decay rapidly from the surface of the body toward the far-field boundary grid points and 2) the grid should not intersect. These conditions are satisfied by defining a different solid mechanics problem, as shown in Fig. 5. The problem involves the domain situated to the exterior of the boundary Γ (defined by the CFD surface grid points), modeled as an infinite elastic and homogeneous medium. The interior of the boundary Γ is treated as a deformable hollow slit. For a given set of deformations of the hollow slit, a straightforward application of the elastostatics BEM equation (7) leads to the desired relationship between the CFD flow-field and surface grid points:

$$\boldsymbol{u}_{a,\text{flowfield grids}} = \boldsymbol{B}' \boldsymbol{u}_{a,\text{surface grids}} \tag{7a}$$

where $\boldsymbol{B}'$ can be derived from Eq. (5) but this time for the external (flowfield) grid points.

From the structural point of view, an intersection of the CFD flowfield grid points would lead to a local stress concentration. However, in the present exterior BEM formulation this cannot happen because the forces are applied only on the boundary Γ. Further, the decay of the deformations away from the body is inherently satisfied because of the infinite medium characteristics.

Results and Discussion

Rigid-Body Motion and Extrapolation

The first set of test cases presented in Fig. 6 deals with the rigid-body displacements of an airfoil represented by the CFD surface grid. The CSD grid is located along a beam-like structure inside

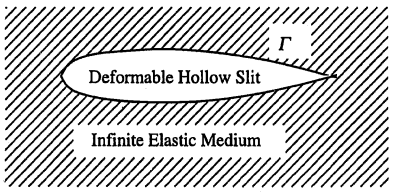

Fig. 5 Exterior BEM problem.

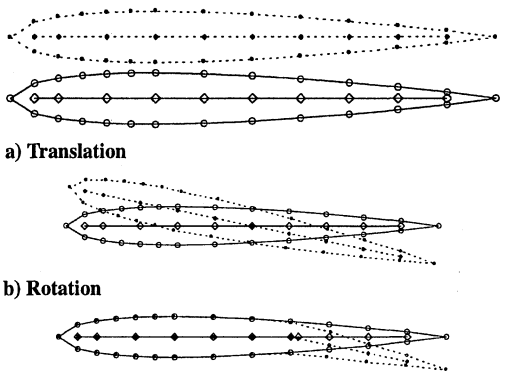

Fig. 6 Rigid-body modes.

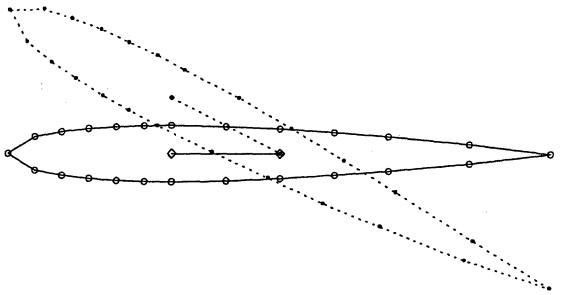

Fig. 7 Accuracy of extrapolation.

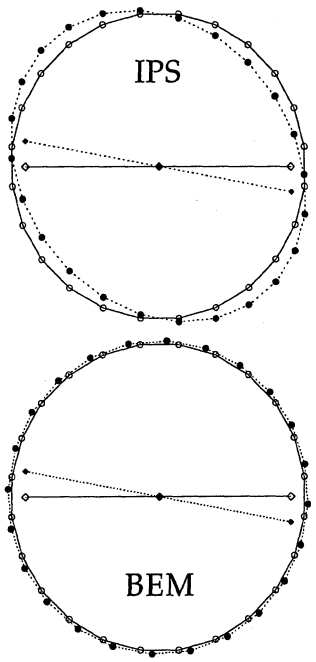

Fig. 8 Circle rotation; IPS/BEM comparison: •, CFD deformed; ○, CFD undeformed; ◇, CSD undeformed; and ♦, CSD deformed.

the airfoil. The solid lines and dashed lines represent the undeformed and deformed positions of the grid points, respectively. The comparisons in Figs. 6a and 6b show that the rigid-body plunging and pitching displacements prescribed at the CSD grid points are perfectly recovered at the CFD surface grid. This is due to the minimum strain energy requirement, which for rigid-body displacements requires the work W [Eq. (9a)] to be zero. The flap deflection case presented in Fig. 6c indicates that the present BEM approach has no problem in recovering the slope discontinuities. Because of the minimum strain energy condition, the elastic deformations are concentrated close to the hinge location, providing a rapid variation of slope at the hinge of the CFD surface grid.

Figure 7 shows a short beam represented by two CSD points located inside an airfoil defined as the CFD grid. For a given pitch deformation at the CSD grid points, large extrapolation regions toward the leading and trailing edges are required. The BEM approach provides a pure rigid-body rotation of the airfoil with no modification of shape, again due to the imposed minimum strain energy condition.

Vector Operator vs Scalar Operator

The cases in Figs. 8 and 9 have been selected to prove the advantage of the present BEM solver over classical scalar methods, such as IPS.[1]

The comparison in Fig. 8 presents a circle defined by the CFD surface grid. A structural beam represented by three points is located along the centerline of the circle. The vertical displacements given at the CSD grid points involve a rigid-body pitch of the beam. This is equivalent to a rigid-body rotation of the circle around its center and, therefore, should lead to a perfect circle result. The BEM method gives the expected result, whereas IPS yields a warped shape. This difference results because the BEM solver is a vector operator whereas IPS is scalar. Because no information concerning

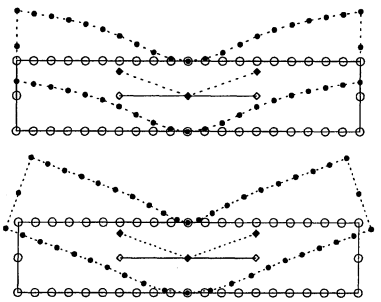

Fig. 9 Rectangular beam bending; IPS/BEM comparison: ○, CFD undeformed; •, CFD deformed; ◇, CSD undeformed; and ♦, CSD deformed.

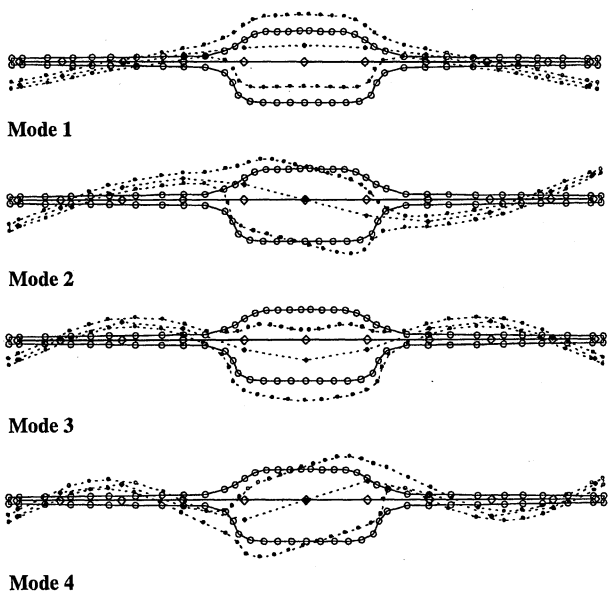

Fig. 10 Blended wing–body configuration: •, CFD deformed; ○, CFD undeformed; ◇, CSD undeformed; and ♦, CSD deformed.

horizontal displacements is provided to the system, IPS does not recover any horizontal displacement at the points located along the vertical diameter. On the other hand, BEM is able to recover horizontal displacements so that the shape of the circle is not altered.

The case of a rectangular beam subjected to a local bending-like deformation is presented in Fig. 9. There are three CSD points located toward the middle of the beam at which the vertical displacements are given so that the structure will bend its tips upward.

It can be observed that the BEM solver preserves the right angles at the corners of the beam, whereas the IPS deforms the corners. Further, the results obtained by BEM solver show a nearly rigid-body pitch motion of the beam outside the central region, where the imposed bending occurs. On the other hand, IPS gives additional bending of the beam toward the tips. Clearly, the correct result is given by the BEM solver because there are no forces acting on the region outside of CSD grid points and, consequently, no curvature of the beam should occur there.

Blended Wing–Body Configuration

A set of cases involving a blended wing–body configuration defined by the CFD surface grid is presented in Fig. 10. The given CSD points are located along an internal beamlike structure extended along the span of the configuration. The results presented in Fig. 10 refer to the first four beam elastic bending modes prescribed at the CSD grid points. Although the relative thickness of the configuration varies greatly, the BEM solver appears to have no problem in recovering the deformation at the CFD surface grid. Further, the results show that the BEM solver can handle wavelike deformations such as high-order structural bending modes.

Force Transformation by the Transpose of the Universal Spline Matrix

The test cases included are meant to prove once more that the BEM solver is robust and can be used in both directions, i.e.,

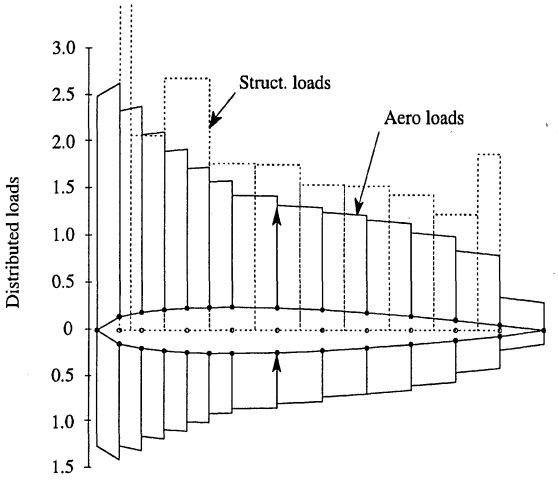

a) Load distribution

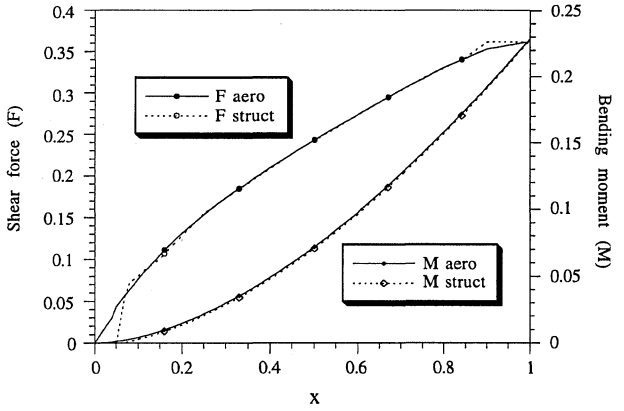

b) Force and moment

Fig. 11 Force transformation comparison for an airfoil: •, at aero grids, and ○, at struct. grids.

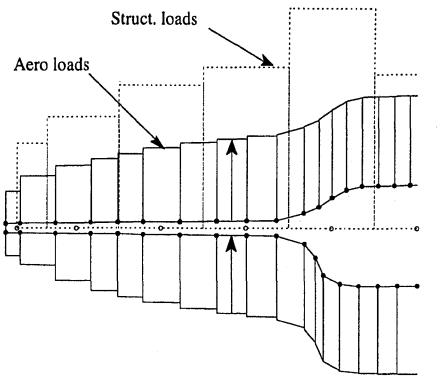

a) Load distribution

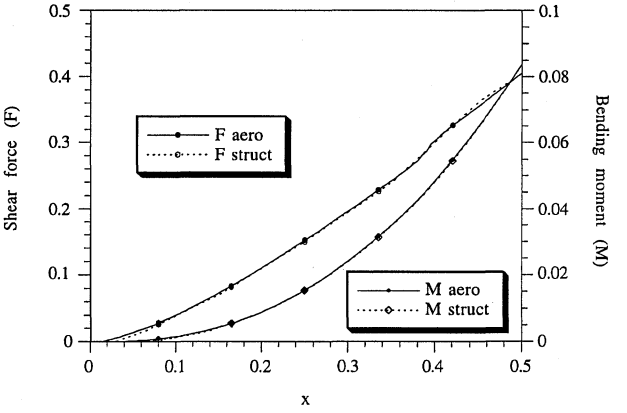

b) Force and moment

Fig. 12 Force transformation comparison for a blended wing–body: •, at aero grids, and ○, at struct. grids.

transforming forces from CFD to CSD [Eq. (2)] and displacements from CSD to CFD grids [Eq. (1)].

Figure 11 presents the transformation of forces from the CFD surface grid on an airfoil to a set of interior points (CSD grid) representing a beam. The given CFD force distributions on the surface are shown with solid lines, and the transformed CSD forces are shown with dashed lines (Fig. 11a). The distributions of forces on the CFD and CSD grids seem to be quite different, especially at the extreme front and aft stations. This is expected because the CFD grid is located on the surface, whereas the CSD grid is located along the internal beam. Furthermore, the internal beam does not extend to the leading and trailing edge of the airfoil. However, the shear force as well as the bending moment distributions integrated from the two sets of distributed loads are in good agreement (Fig. 11b). It must be observed that the shear force and bending moment at the trailing edge represent the global loads acting on the airfoil, and their good agreement indicates that the BEM solver satisfies the conservation of loads. Therefore, there is no loss of global information during the force transformation.

A similar case referring to a blended wing–body configuration is presented in Fig. 12. The loads are given on the CFD grid located on the surface of the configuration. The CSD grid points where the loads need to be transformed are located on a beam inside the configuration (Fig. 12a). Once more, the shear force and bending moment of the CFD and CSD force distributions are in good agreement (Fig. 12b).

Based on the two cases presented, we believe that the BEM solver provides a level of accuracy of the force transformation that subsequently enables a reliable stress analysis of the structure.

CFD Flowfield Grid Deformation by Exterior BEM Solver

Figure 13 presents a typical flowfield mesh for the CFD analysis of an airfoil section. For a given displacement of the airfoil surface, it is required to find a corresponding smoothly deformed flowfield grid.

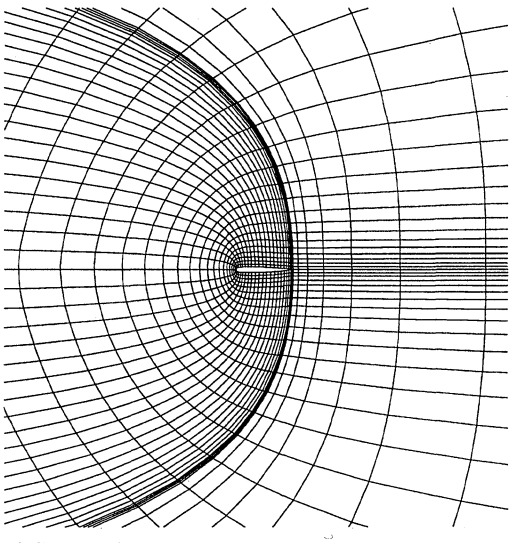

a) General view

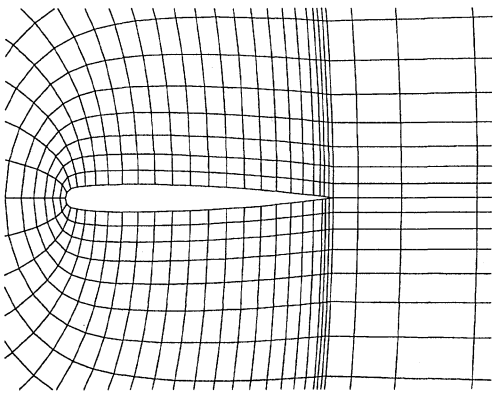

b) Detail

Fig. 13 Undeformed CFD grid.

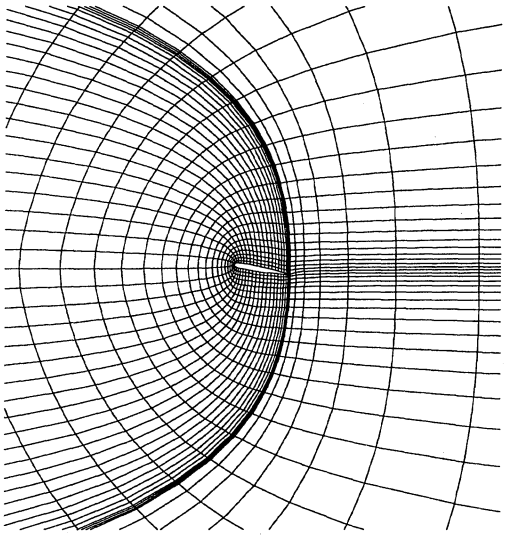

a) General view

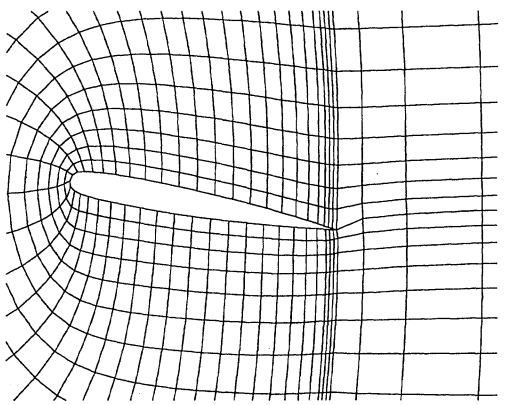

b) Detail

Fig. 14 Deformed CFD grid.

For a given rigid-body pitching deformation prescribed on the airfoil surface, the deformed flowfield grid obtained by the exterior BEM solver is presented in Figs. 14a and 14b. By comparing Figs. 13a and 14a, it can be observed that there is virtually no deformation of the grid points at large distances from the airfoil. Further, from Fig. 14b it can be seen that the transition of the deformation from near-field to far-field grid points is smooth and no grid intersections appear. Finally, the $\boldsymbol{B}'$ matrix in Eq. (7a) is invariant during the CFD/CSD iterations, making the exterior BEM solver an efficient tool for deformed grid generation.

Conclusions

The CFD/CSD interfacing is fundamentally a solid mechanics problem. Therefore, any attempts to solve for the grid topologies or to improve the existing spline methods alone are likely to be ad hoc methods, as opposed to the unified features of the present BEM solver.

Central in the present BEM techniques, the BEM solver yields proper structural deformations of the CFD grid points. Hence, extrapolation is not an issue.

The present BEM solver is fully automated, requiring minimum user interaction, and relies exclusively on the existing CFD and CSD discretizations, whereby no additional model is necessary. The BEM solver admits discontinuities in slope and is applicable to all CFD grid systems in that it accepts both structured and unstructured grids; hence, it could adopt the existing graphics capabilities.

As an operator on the grid systems, the universal spline matrix is independent of the CSD displacements and CFD forces. It is established once and for all and is invariant during the time-marching procedure. Therefore, it is ideally suitable for CAE and multidisciplinary optimization applications.

The current CFD methods have reached their maturity, calling for an effective three-dimensional CFD/CSD interfacing methodology. One such methodology is likely to be the present BEM solver.

References

[1]Harder, R. L., and Desmarais, R. N., "Interpolation Using Surface Splines," *AIAA Journal*, Vol. 9, No. 2, 1972, pp. 189–191.

[2]Done, G. T. S., "Interpolation of Mode Shapes: A Matrix Scheme Using Two-Way Spline Curves," *Aeronautical Quarterly*, Vol. 16, Nov. 1965, pp. 333–349.

[3]Giesing, J. P., Kalman, T. P., and Rodden, W. P., "Subsonic Steady and Oscillatory Aerodynamics for Multiple Interfering Wings and Bodies," *Journal of Aircraft*, Vol. 9, No. 10, 1972, pp. 693–702.

[4]Appa, K., "Finite Surface Splines," *Journal of Aircraft*, Vol. 26, No. 5, 1989, pp. 495, 496.

[5]Duchon, J., "Splines Minimizing Rotation-Invariant Semi-Norms in Sobolev Spaces," *Constructive Theory of Functions of Several Variables*, edited by W. Schempp and K. Zeller, Springer, Oberwolfach, Germany, 1976, pp. 85–100.

[6]Hardy, R. L., "Theory and Applications of the Multiquadric Biharmonic Method," *Computers and Mathematics with Applications*, Vol. 19, No. 8/9, 1990, pp. 163–208.

[7]Smith, M. J., Cesnik, C. E. S., Hodges, D. H., and Moran, K. J., "An Evaluation of Computational Algorithms to Interface between CFD and CSD Methodologies," AIAA Paper 96-1400, 1996.

[8]Hounjet, M. H. L., and Meijer, J. J., "Evaluation of Elastomechanical and Aerodynamic Data Transfer Methods for Non-planar Configurations in Computational Aeroelastic Analysis," *Proceedings of the International Forum on Aeroelasticity and Structural Dynamics* (Manchester, England, UK), Royal Aeronautical Society, 1995, pp. 10.1–10.25.

[9]Petiau, C., and Nicot, P., "A General Method for Mathematical Model Identification in Aeroelasticity," *Proceedings of the International Forum on Aeroelasticity and Structural Dynamics*, 1995, pp. 67.1–67.9.

[10]Guruswamy, G. P., "Coupled Finite-Difference/Finite-Element Approach for Wing–Body Aeroelasticity," AIAA Paper 92-4680, 1992.

[11]Batina, J. T., "Unsteady Euler Algorithm with Unstructured Dynamic Mesh for Complex-Aircraft Aeroelastic Analysis," *AIAA Journal*, Vol. 29, No. 3, 1991, pp. 327–333.

[12]Brebbia, C. A., and Dominguez, J., *Boundary Elements: An Introductory Course*, McGraw–Hill, New York, 1992, Chap. 3.

R. K. Kapania
Associate Editor